

# Mitochondrial DNA Mutations Increase in Early Stage Alzheimer Disease and Are Inconsistent with Oxidative Damage

Jake G. Hoekstra, PhD,<sup>1</sup>  
 Michael J. Hipp, BS,<sup>1</sup>  
 Thomas J. Montine, MD, PhD,<sup>2</sup> and  
 Scott R. Kennedy, PhD<sup>1</sup>

Mitochondrial dysfunction and oxidative damage are commonly associated with early stage Alzheimer disease (AD). The accumulation of somatic mutations in mitochondrial DNA (mtDNA) has been hypothesized to be a driver of these phenotypes, but the detection of increased mutation loads has been difficult due to a lack of sensitive methods. We used an ultrasensitive next generation sequencing technique to measure the mutation load of the entire mitochondrial genome. Here, we report a significant increase in the mtDNA mutation frequency in the hippocampus of early stage AD, with the cause of these mutations being consistent with replication errors and not oxidative damage.

ANN NEUROL 2016;80:301–306

Somatic (noninherited) mitochondrial DNA (mtDNA) mutations and mitochondrial dysfunction are thought to be important drivers of aging and age-related neurodegenerative diseases such as Alzheimer disease (AD) and Parkinson disease (PD), where mtDNA mutation accumulation may precede the appearance of clinical symptoms.<sup>1</sup> Mutations in mtDNA, whether through inheritance or somatic accumulation, can compromise mitochondrial function and result in cell death and disease.<sup>2,3</sup> Previous studies investigating the contributions of mtDNA mutations in AD have failed to consistently identify associations between AD and mutations.<sup>4,5</sup> Such inconsistencies likely stem from 3 main causes: (1) the inclusion of only samples from patients with late stage AD, wherein only the healthiest cells with the lowest mutation loads likely remain; (2) the examination of relatively small regions in mtDNA; and (3) the use of polymerase chain reaction (PCR) amplification techniques that result in higher error rates due to misincorporation events by DNA polymerase.

To overcome these issues, we examined point mutations and small insertions/deletions across the entire mitochondrial genome purified from the hippocampus and parietal lobe of AD, early stage AD, and healthy control patients using duplex sequencing (DS). DS is a highly accurate next generation sequencing (NGS) methodology that relies on molecular barcoding and sequencing of both strands of a double-stranded DNA molecule to eliminate both sequencer- and PCR-derived errors, thus allowing for the detection of a single mutation in  $>10^7$  wild-type nucleotides (Fig 1A–C).<sup>6,7</sup>

## Materials and Methods

### Human Brain Samples

Flash frozen brain tissue was obtained from the Neuropathology Core of the University of Washington Alzheimer's Disease Research Center (Seattle, WA). All clinical information and consent were obtained according to protocols approved by the University of Washington Institutional Review Board (IRB#24250). Cases were grouped using 2 criteria: last clinical diagnosis of no dementia (ND, within 2 years of death) or dementia (D) according to criteria from the Diagnostic and Statistical Manual of Mental Disorders, 4th edition and pathologic classification for AD by Braak staging<sup>8</sup>; cases with any other neuropathologic diagnosis, gross infarcts/hemorrhages, Lewy bodies, or ischemic injury were excluded. We stratified cases into 3 groups: no dementia and Braak none, I, or II (ND/Low-AD); no dementia and Braak III, IV (ND/High-AD); and AD dementia with Braak stage V or VI (D/High-AD; Table, Supplementary Table 1).

### Isolation of Synaptosomes and mtDNA from Human Brain Tissue

In an effort to enrich for mtDNA from neurons, we isolated synaptosomes from 100 to 200mg of tissue from each case using a previously established protocol.<sup>9</sup> Purity of the resulting synaptosome fraction was evaluated by Western blot analysis using antibodies against glial fibrillary acidic protein (Dako, Carpinteria, CA) and synaptophysin (Dako; see Fig 1D). DNA was extracted from the synaptosome pellet using the QIAamp DNA Micro kit (Qiagen, Valencia, CA), following instructions

From the <sup>1</sup>Department of Pathology, University of Washington, Seattle, WA; and <sup>2</sup>Department of Pathology, Stanford University, Palo Alto, CA.

Address correspondence to Dr Kennedy, HSB E506, Box 357470, 1959 NE Pacific St, Seattle, WA 98195. E-mail: scottrk@uw.edu

Additional supporting information can be found in the online version of this article

Received Mar 8, 2016, and in revised form Jun 13, 2016. Accepted for publication Jun 15, 2016.

View this article online at [wileyonlinelibrary.com](http://wileyonlinelibrary.com). DOI: 10.1002/ana.24709

for tissue isolation. The relative purity of each mtDNA preparation was determined by quantitative PCR (qPCR) using the following primers sets: nuclear primers: forward, 5'GGGCACTGATCTACACAGTAAG3'; reverse, 5'TAGTAAGCGCTCAGCAAAGG3'; mitochondrial primers; forward, 5'CCTCAACAGTTAAATCAACAA3'; reverse, 5'GCGCTTACTTTGTAGCCTTCA3'.

### mtDNA Duplex Sequencing and Data Analysis

Duplex tag-labeled adapter synthesis and DNA shearing were performed as previously described.<sup>7,10</sup> Briefly, adapters (see Fig 1A) were ligated to sheared DNA using NEBNext Ultra End Repair/da-Tailing and Ligation modules (New England BioLabs, Ipswich, MA) according to the manufacturer's instructions. Approximately  $1 \times 10^6$  copies of adapter ligated mtDNA (determined by qPCR) were PCR amplified using KAPA HiFi DNA polymerase (Kapa Biosystems, Wilmington, MA). The DNA was then used in targeted capture using IDT xGen Lockdown probes (Integrated DNA Technologies, Coralville, IA) specific for human mtDNA following the manufacturer's instructions. The resulting libraries were sequenced using 101-base pair (bp) paired-end reads on an Illumina (San Diego, CA) HiSeq 2500.

The raw sequencing data were processed as previously described.<sup>10</sup> A minimum of  $1 \times 10^6$  postprocessing bases were required for each sample. To quantify the frequency of de novo events, we used a clonality cutoff excluding any positions with variants occurring at a heteroplasmic level of  $>1\%$  or a depth of  $<100\times$ , and scored each type of mutation only once at each genome position (Supplementary Table 2).

### Statistics

Statistical significance of mutation frequencies between each disease group and control patients was assessed using an unpaired *t* test. To adjust for 3 pairwise comparisons (ND/High-AD vs ND/Low-AD, ND/High-AD vs D/High-AD, and ND/Low-AD vs D/High-AD), Bonferroni correction was applied and significance was set at  $p = 0.017$ .

### Results

Tissue from the hippocampus and parietal lobe were obtained for controls (ND/Low-AD), patients with AD dementia (D/High-AD), and individuals who were not demented, but had high Braak staging characteristic of AD dementia (ND/High-AD; see Supplementary Table 1). This last group does not have neuronal loss; subjects are cognitively normal, but are thought to be at risk of developing AD dementia, thus representing an early stage of AD.<sup>11</sup>

Purification of total DNA from bulk brain tissue indicated a significantly reduced amount of mtDNA in the D/High-AD group relative to both the ND/Low-AD and the ND/High-AD groups (see Fig 1E), consistent with previous studies showing a reduction in mtDNA amounts in cerebrospinal fluid.<sup>12</sup> As AD primarily affects neurons, we next sought to measure the mutation frequency of neuronally derived mtDNA by isolating

hippocampal synaptosomes via a Percoll step-gradient centrifugation strategy and then assessing the somatic mtDNA mutation frequency using DS. The mutation frequency of mtDNA from ND/Low-AD control hippocampal samples was  $1.69 \pm 0.32 \times 10^{-5}$ , in close agreement with previous reports,<sup>6</sup> whereas the mutation frequency of ND/High-AD samples exhibited a  $\sim 60\%$  increase ( $2.77 \pm 0.35 \times 10^{-5}$ ,  $p = 0.0009$ ; Fig 2A). No significant increase was detected in D/High-AD cases, or other brain regions (see Fig 2A, B). Small insertion/deletions ( $<5\text{bp}$ ) were slightly increased in the hippocampus of the ND/High-AD group (see Fig 2C,  $p = 0.009$ ), but not the D/High-AD group. In assessing differences between the characteristics of the groups, no significant differences were observed between postmortem intervals of any group (see Table). When considering age, the D/High-AD group was significantly younger than the ND/High-AD group ( $p = 0.017$ , Student *t* test), and trended lower than the ND/Low-AD controls ( $p = 0.032$ , Student *t* test). However, age did not significantly correlate with mutation frequency in either the hippocampus ( $r^2 = 0.018$ ,  $df = 13$ ,  $p = 0.64$ , Pearson correlation) or parietal lobe ( $r^2 = 0.053$ ,  $df = 11$ ,  $p = 0.44$ , Pearson correlation), indicating that the lower sample age in the D/High-AD samples is unlikely to account for the reduced mutation frequency observed in that sample group.

Oxidative damage to mtDNA has been reported to be increased in several stages related to AD dementia.<sup>13–15</sup> The most frequent DNA alteration produced by oxidative damage is 8-hydroxy-2'-deoxyguanosine, which, when copied past during replication or repair, yields G→T/C→A transversions.<sup>16</sup> Surprisingly, we found no significant increase in this mutation subtype in the hippocampus or the parietal lobe of any sample group (see Fig 2E, F), suggesting that regional differences in the brain may not account for our observations. Instead, T→C/A→G and G→A/C→T transitions were the most common mutation subtypes observed in all samples, with these subtypes being increased in the ND/High-AD sample group (see Fig 2E, F). These findings are consistent with recent reports showing that transitions and not oxidative damage-associated G→T/C→A mutations increase in brain tissue with age.<sup>6,17</sup>

The occurrence of mutations were dispersed throughout the genome, with a  $\sim 3$ - to 4-fold elevation in the mutation load in the regulator D-loop (see Fig 2D; positions: 1–576; 16,024–16,569) compared to the coding regions (positions: 577–16,023), consistent with previous work.<sup>6</sup> However, comparison of the relative increase in the mutation frequency of the D-loop versus the coding region of the ND/Low-AD and ND/High-AD groups shows no significant change in the

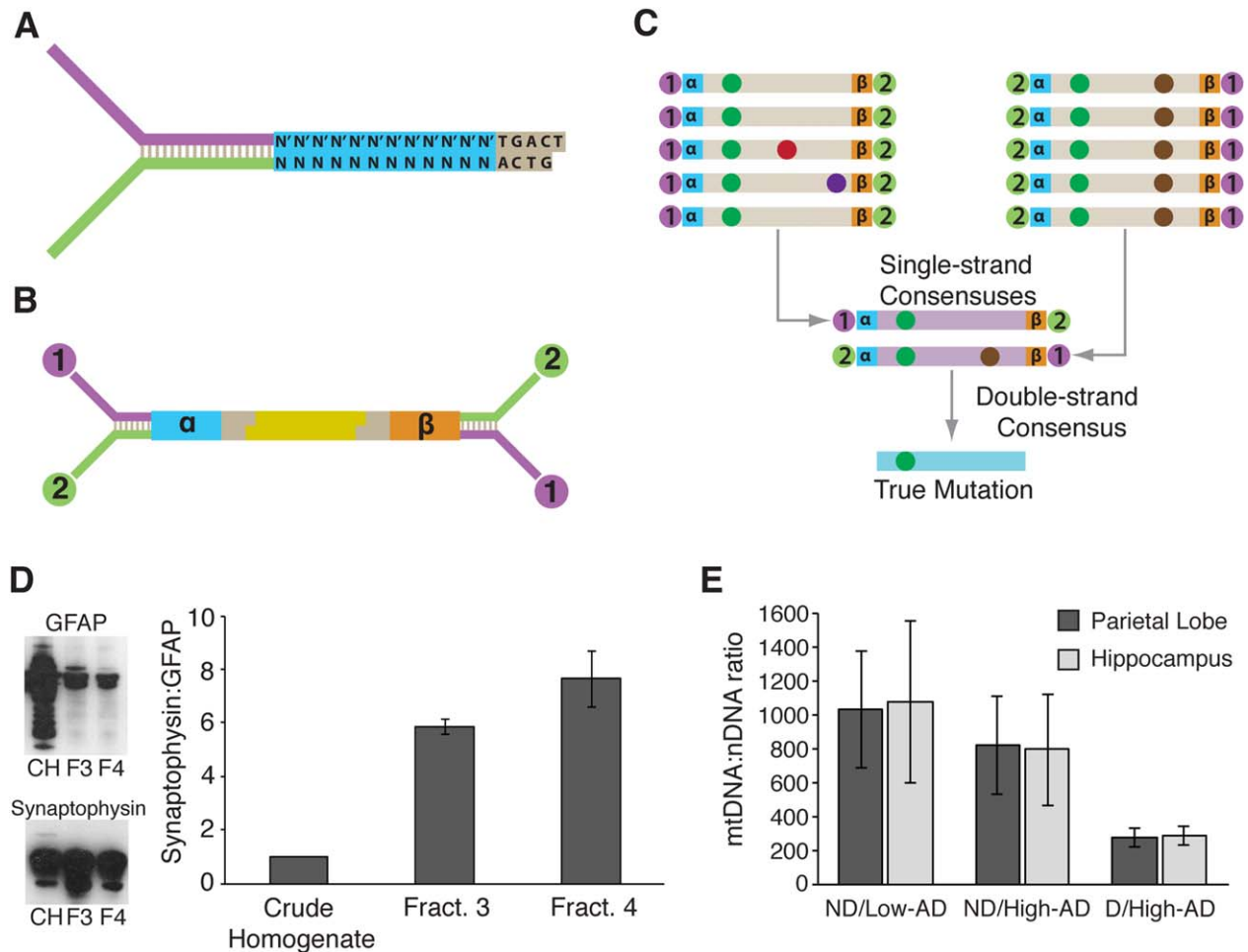


**FIGURE 1:** Overview of Duplex Sequencing and sample purity. (A) Duplex Sequencing uses a modified form of the Illumina TruSeq adapter design containing a unique complementary random sequence. (B) Ligation of the adapters to sheared DNA (yellow) generates unique tags on each end ( $\alpha$  and  $\beta$ ), such that each molecule has a different tag combination. Reads derived from the read 1 and read 2 synthesis reactions of a paired-end run are denoted in purple and green, respectively. (C) Polymerase chain reaction (PCR) amplification of the 2 strands produces 2 related, but distinct products. Sequence reads sharing the same  $\alpha$  and  $\beta$  combination and the same sequencing reaction (ie, read 1 or read 2) are grouped into "families A consensus sequence for each family is then calculated to form a "single-strand consensus" sequence (SSCS) using a simple majority rules consensus caller. Putative mutations are of 3 different types: sequencing mistakes or late arising PCR errors (red and purple spots); first round PCR errors (brown spots); and true mutations (green spots). Formation of the SSCS removes sequencer mistakes and late arising PCR errors, but is unable to remove first round PCR errors. Comparison of the SSCS with appropriately oriented  $\alpha$  and  $\beta$  tags derived from the complementary strands of the original double-stranded DNA generates a double-strand consensus. Figure is adapted from Kennedy et al.<sup>6</sup> (D) Synaptosome fractionation increases the purity of neuronally derived mitochondria. Synaptosomes were purified from crude homogenized brain tissue using a Percoll step gradient fractionation protocol provided by Dunkley et al.<sup>9</sup> Only Percoll fraction 4 was used for sequencing due to a significant enrichment in mitochondrial DNA (mtDNA) being found in this fraction. Panel includes representative Western blots of glial fibrillary acidic protein (GFAP; top) and synaptophysin (bottom), as well as the quantification of the Western blots for normal hippocampus. CH = crude homogenate, F3 = Percoll fraction 3, F4 = Percoll fraction 4. (E) Reduced mtDNA content in dementia D/High-AD sample group in both the hippocampus and parietal lobe. Only D/High-AD shows a reduced amount of mtDNA, suggesting that a significant portion of mitochondria are no longer present in advanced dementia. Error bars indicate 1 standard deviation. ND = no dementia.

distribution of mutations between these 2 mtDNA regions (see Fig 2D), indicating that mutation accumulation does not occur to a different extent in the D-loop compared to the genome's coding region.

## Discussion

Utilizing a highly sensitive NGS technique that eliminates sequencing errors associated with PCR and DNA

damage, we have measured the mutation frequency of neuronally enriched mtDNA from patients with varying stages of AD pathology at sensitivities previously unachievable. Compared to controls, the mtDNA point mutation frequency is significantly elevated in the hippocampus of patients with early stage AD, but not in patients with pathologically confirmed AD dementia, suggesting that mutated mtDNA may be lost as neurons

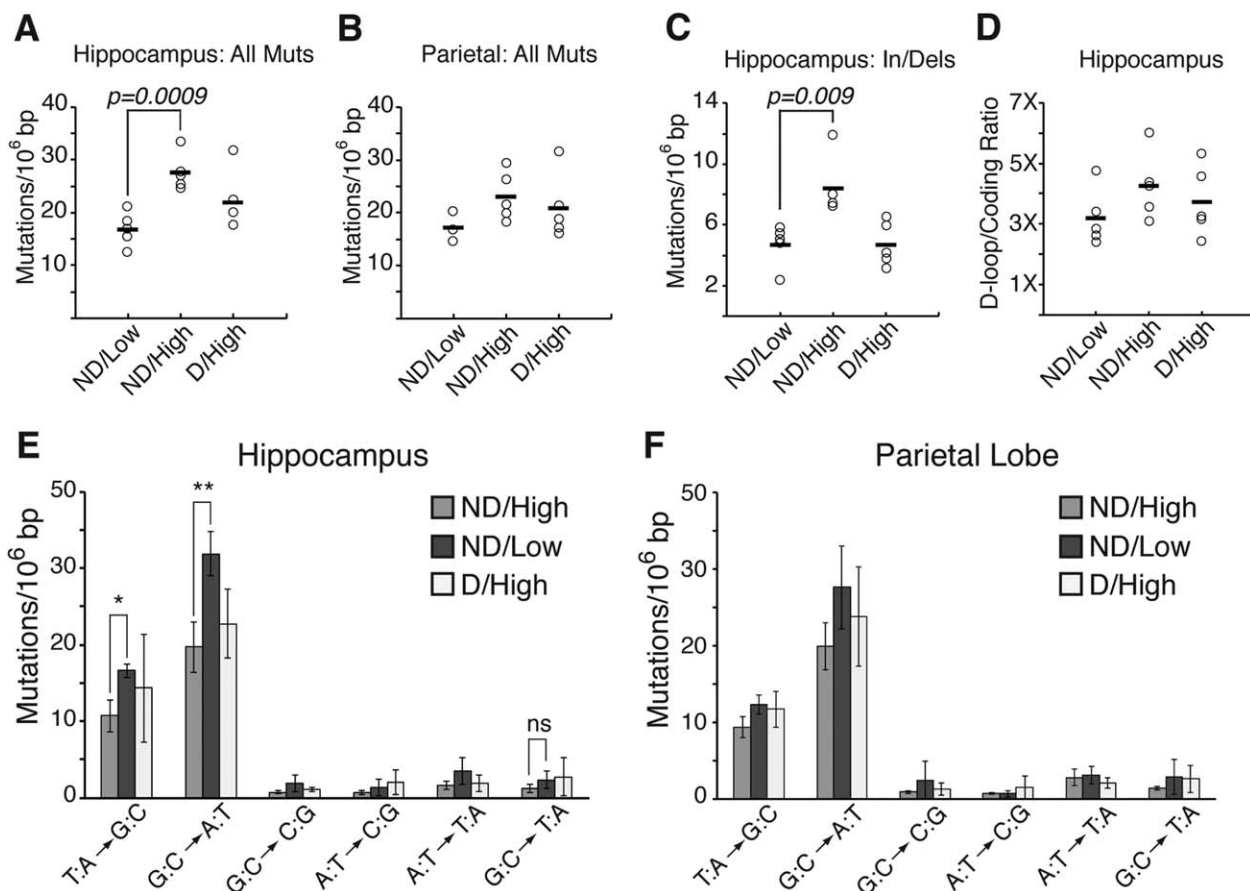


**FIGURE 2:** Somatic mitochondrial DNA (mtDNA) mutation levels in no dementia (ND)/low Alzheimer disease (AD) controls (ND/Low-AD), early stage AD (ND/High-AD), and Alzheimer dementia (D/High-AD). mtDNA was extracted from synaptosomes purified by ultracentrifugation with a Percoll gradient. The DNA was then sequenced using Duplex Sequencing, as previously described.<sup>10</sup> (A) Overall somatic point mutation frequency in hippocampus. The thick black bars indicate the mean. (B) Overall somatic point mutation frequency in parietal lobe. (C) Overall somatic frequency of insertions and deletions (In/Dels) in the hippocampus. (D) The D-loop harbors  $\sim 4 \times$  more mutations than the coding regions of the mtDNA, but the ratio is unchanged between the normal and disease states. (E) Mutation spectrum reveals a predominance of T:A→G:C and G:C→A:T transitions that are elevated in ND/High-AD, but not D/High-AD. G:C→T:A transversions are in low abundance and are unchanged with respect to disease state. \* $p = 0.0004$ ; \*\* $p = 0.0002$ ; ns = not significant. (F) Mutation spectrum for the parietal lobe reveals that transition mutations are the predominant mutation type.

die and the disease progresses. This idea is consistent with our observation that the mtDNA:nDNA ratio is dramatically reduced in our D/High-AD samples (see Fig 1E).

Oxidative stress is prevalent in AD and has been hypothesized to be a driving force behind the onset and progression of the disease. Although elevated oxidative damage

**TABLE. Sample Characteristics**

Disease State	ND/Low-AD	ND/High-AD	D/High-AD
Age, yr, mean $\pm$ SD	85.8 $\pm$ 4.76	88.8 $\pm$ 5.76	69.2 $\pm$ 13.5
Sex, M/F	1/4	4/1	2/3
PMI, h, mean $\pm$ SD	6.03 $\pm$ 2.30	4.92 $\pm$ 1.59	5.33 $\pm$ 1.33
Age at onset, yr, mean $\pm$ SD	N/A	N/A	60.6 $\pm$ 10.64
Disease duration, yr, mean $\pm$ SD	N/A	N/A	8.6 $\pm$ 3.91

D = dementia; F = female; M = male; N/A = not applicable; ND = no dementia; PMI = postmortem interval; SD = standard deviation.

to mtDNA is a feature of AD and is observed at several stages that precede clinical presentation,<sup>13–15</sup> we did not observe an elevation in G→T/C→A mutations, a canonical signature of oxidative damage to DNA. Instead, we note an increase in transitions, which primarily result from nucleotide deamination or nucleotide misincorporation by DNA polymerase  $\gamma$  during mtDNA replication.<sup>18,19</sup> Interestingly, deficiencies in replication fidelity and impaired removal of defective mitochondria, have been reported in AD, suggesting a potential origin for the increase in mtDNA mutation load.<sup>20,21</sup>

Our findings are in contrast to previous studies in early PD and incidental Lewy body disease that report a large increase in G→T/C→A mutations.<sup>23</sup> This striking contrast points to an underlying difference in the etiologies of AD and PD and suggests that, unlike early PD, mitochondrially localized oxidative stress may not be an early contributor to AD. Alternatively, the discordance between our findings and earlier reports could be explained by their use of PCR-based assays, which can lead to erroneous misincorporation events, to quantify mutations. Consistent with this possibility is that the mutation frequencies we report here are ~10-fold lower than those reported in these studies,<sup>5,23</sup> and are in closer agreement with previous studies in humans.<sup>6</sup>

Our data suggest that mtDNA mutations either contribute to the onset of AD or indicate an early change in neuronal mitochondria of AD patients. The similarity of the mutation spectra between the different sample groups suggests a similar mutagenic process, which may represent an “enhanced aging” phenotype in patients with AD pathology. Taken together, our findings may prove useful in the future as a potential biomarker and suggest a potential therapeutic strategy that prevents and/or targets the accumulation of mtDNA mutations in AD.

## Acknowledgment

This research was supported by the University of Washington Alzheimer’s Disease Research Center (NIH P50AG05136) and a Genetic Approaches to Aging Training Grant (NIH National Institute on Aging T32-AG000057, S.R.K.). The funders had no role in study design, data collection and analysis, decision to publish, or preparation of the manuscript.

We thank Drs L. Loeb and A. Herr for their critical review of the manuscript.

## Author Contributions

S.R.K., T.J.M., and J.G.H. conceived and designed the project. S.R.K., J.G.H., and M.J.H. collected, analyzed, and interpreted data. S.R.K. and J.G.H. wrote the paper.

## Potential Conflicts of Interest

Nothing to report.

## References

- Kennedy SR, Loeb LA, Herr AJ. Somatic mutations in aging, cancer and neurodegeneration. *Mech Ageing Dev* 2012;133:118–126.
- Hayashi J, Ohta S, Kikuchi A, et al. Introduction of disease-related mitochondrial DNA deletions into HeLa cells lacking mitochondrial DNA results in mitochondrial dysfunction. *Proc Natl Acad Sci U S A* 1991;88:10614–10618.
- Mashima Y, Saga M, Hiida Y, et al. Quantitative determination of heteroplasmy in Leber’s hereditary optic neuropathy by single-strand conformation polymorphism. *Invest Ophthalmol Vis Sci* 1995;36:1714–1720.
- Coskun PE, Beal MF, Wallace DC. Alzheimer’s brains harbor somatic mtDNA control-region mutations that suppress mitochondrial transcription and replication. *Proc Natl Acad Sci U S A* 2004;101:10726–10731.
- Lin MT, Simon DK, Ahn CH, et al. High aggregate burden of somatic mtDNA point mutations in aging and Alzheimer’s disease brain. *Hum Mol Genet* 2002;11:133–145.
- Kennedy SR, Salk JJ, Schmitt MW, Loeb LA. Ultra-sensitive sequencing reveals an age-related increase in somatic mitochondrial mutations that are inconsistent with oxidative damage. *PLoS Genet* 2013;9:e1003794.
- Schmitt MW, Kennedy SR, Salk JJ, et al. Detection of ultra-rare mutations by next-generation sequencing. *Proc Natl Acad Sci U S A* 2012;109:14508–14513.
- Braak H, Braak E. Neuropathological stageing of Alzheimer-related changes. *Acta Neuropathol* 1991;82:239–259.
- Dunkley PR, Jarvie PE, Robinson PJ. A rapid Percoll gradient procedure for preparation of synaptosomes. *Nat Protoc* 2008;3:1718–1728.
- Kennedy SR, Schmitt MW, Fox EJ, et al. Detecting ultralow-frequency mutations by duplex sequencing. *Nat Protoc* 2014;9:2586–2606.
- Nelson PT, Braak H, Markesbery WR. Neuropathology and cognitive impairment in Alzheimer disease: a complex but coherent relationship. *J Neuropathol Exp Neurol* 2009;68:1–14.
- Podlesniy P, Figueiro-Silva J, Llado A, et al. Low cerebrospinal fluid concentration of mitochondrial DNA in preclinical Alzheimer disease. *Ann Neurol* 2013;74:655–668.
- Lovell MA, Soman S, Bradley MA. Oxidatively modified nucleic acids in preclinical Alzheimer’s disease (PCAD) brain. *Mech Ageing Dev* 2011;132:443–448.
- Wang J, Xiong S, Xie C, et al. Increased oxidative damage in nuclear and mitochondrial DNA in Alzheimer’s disease. *J Neurochem* 2005;93:953–962.
- Wang J, Markesbery WR, Lovell MA. Increased oxidative damage in nuclear and mitochondrial DNA in mild cognitive impairment. *J Neurochem* 2006;96:825–832.
- Cheng KC, Cahill DS, Kasai H, et al. 8-Hydroxyguanine, an abundant form of oxidative DNA damage, causes G→T and A→C substitutions. *J Biol Chem* 1992;267:166–172.
- Williams SL, Mash DC, Züchner S, Moraes CT. Somatic mtDNA mutation spectra in the aging human putamen. *PLoS Genet* 2013;9:e1003990.
- Duncan BK, Miller JH. Mutagenic deamination of cytosine residues in DNA. *Nature* 1980;287:560–561.

19. Zheng W, Khrapko K, Coller HA, et al. Origins of human mitochondrial point mutations as DNA polymerase gamma-mediated errors. *Mutat Res* 2006;599:11–20.
20. Alvarez V, Corao AI, Alonso-Montes C, et al. Mitochondrial transcription factor A (TFAM) gene variation and risk of late-onset Alzheimer's disease. *J Alzheimers Dis* 2008;13:275–280.
21. Wang X, Su B, Lee H, et al. Impaired balance of mitochondrial fission and fusion in Alzheimer's disease. *J Neurosci* 2009;29:9090–9103.
22. Lin MT, Cantuti-Castelvetri I, Zheng K, et al. Somatic mitochondrial DNA mutations in early Parkinson and incidental Lewy body disease. *Ann Neurol* 2012;71:850–854.